

# Altered reward-related effective connectivity in obsessive-compulsive disorder: an fMRI study

Ana Alves-Pinto, PhD; Oana Georgiana Rus, PhD; Tim Jonas Reess, PhD; Afra Wohlschläger, PhD; Gerd Wagner, PhD; Götz Berberich, MD; Kathrin Koch, PhD

Published online on Apr. 9, 2019; subject to revision

**Background:** Obsessive–compulsive disorder (OCD) is characterized by anxiety-provoking, obsessive thoughts. Patients usually react to these thoughts with repetitive behaviours that reduce anxiety and are perceived as rewarding. Hence, reward plays a major role in the psychopathology of OCD. Previous studies showed altered activation in frontostriatal networks, among others, in association with the processing of reward in patients with OCD. Potential alterations in connectivity within these networks have, however, barely been explored. **Methods:** We investigated a sample of patients with OCD and healthy controls using functional MRI and a reward learning task presented in an event-related design. Dynamic causal modelling (DCM) was used to estimate effective connectivity. **Results:** Our sample included 37 patients with OCD and 39 healthy controls. Analyses of task-related changes in connectivity showed a significantly altered effective connectivity between the ventromedial prefrontal cortex (vmPFC) and the orbitofrontal cortex (OFC), among others, both in terms of endogenous connectivity as well as modulatory effects under positive feedback. Clinical measures of compulsion correlated with the effect of feedback input on visual sensory areas. **Limitations:** The reported alterations should be interpreted within the context of the task and the a priori–defined network considered in the analysis. **Conclusion:** This disrupted connectivity in parts of the default mode network and the frontostriatal network may indicate increased rumination and self-related processing impairing the responsiveness toward external rewards. This, in turn, may underlie the general urge for reinforcement accompanying compulsive behaviours.

## Introduction

Obsessive–compulsive disorder (OCD) is characterized by anxiety-provoking, obsessive thoughts (i.e., obsessions), which patients react to with repetitive behaviours (i.e., compulsions) to counteract anxiety. Patients perceive their obsessive thoughts as involuntary and uncontrollable. Reactive compulsive behaviours, in turn, are often perceived as addictive and remunerating because of their rewarding impact after reducing obsession-related anxiety. Hence, reward plays a central role in the psychopathology of OCD.

Another link between OCD and reward is that current neuroanatomical models of both reward processing and OCD are based on functional loops involving, among others, frontostriatal networks including lateral and medial orbitofrontal cortices.<sup>1,2</sup> Key regions of the frontostriatal system in the context of reward processing contain the striatum and the orbitofrontal cortex (OFC). The ventral part of the striatum (i.e., nucleus accumbens) is known to be strongly involved in the processing of rewarding stimuli.<sup>3</sup> Studies showing that the ventral striatum/nucleus accumbens is a successful target

for deep brain stimulation in the treatment of OCD highlight the psychopathological relevance of this structure in the context of OCD.<sup>4–6</sup>

Thus, areas and networks involved in the processing of reinforcement and reward correspond to frontostriatal networks that are known to be of major psychopathological relevance for OCD.<sup>7</sup> In line with this congruence, a growing number of studies report altered frontostriatal involvement in OCD in association with the processing of reinforcement and reward. Jung and colleagues<sup>8</sup> reported increased activation in a frontostriatal network during reward outcome as well as an increased ventral–striatal activation when comparing no-loss versus loss outcomes between patients with OCD and healthy controls. Figeo and colleagues<sup>9</sup> could not find any activation differences between the groups during reward outcome, but they observed reduced activity in the ventral striatum during reward anticipation in patients with OCD compared with healthy controls.

Activation alterations in association with reward anticipation in OCD were also reported in a study by Kaufman and colleagues.<sup>10</sup> In that study, patients exhibited increased

**Correspondence to:** A. Alves-Pinto, Department of Orthopedics and Sports Orthopedics, School of Medicine, Klinikum rechts der Isar, Technical University of Munich, Ismaningerstr 22, 81675 Munich, Bavaria, Germany; ana.alves-pinto@tum.de

Submitted Oct. 18, 2018; Revised Jan. 16, 2019; Accepted Jan. 28, 2019

DOI: 10.1503/jpn.180195

activation in association with the anticipation of punishment and decreased activation in association with the anticipation of reward in mainly medial and superior frontal regions.

In addition, decreased responsiveness in the OFC and dorso-ventral striatum regions has been reported in patients with OCD during reward outcome in the context of reinforcement-based reversal learning.<sup>11</sup> In a reward-based spatial learning task,<sup>12</sup> patients with OCD failed to activate the striatum (i.e., ventral putamen) and amygdala during reward anticipation or the hippocampus, amygdala and striatum (i.e., putamen) during reward outcome.

In sum, there is a growing body of evidence for altered activation predominantly in the dorsal and ventral striatum and orbitofrontal cortex in patients with OCD in association with the processing of reward (anticipation v. positive/negative outcome), even though findings must be regarded as rather heterogeneous. Nonetheless, the observation of structural alterations in areas beyond frontostriatal circuits (as highlighted in a recent review by Piras and colleagues<sup>13</sup>) suggests that changes in network dynamics in patients with OCD are likely widespread. In particular, circuits associated with executive functions, such as prefrontal cortices, as well as frontosubcortical circuits may also be involved, contributing further to increase the palette and complexity of OCD symptomatology.

Despite the fact that — from a functional perspective — there are reasonable grounds to assume that alterations in activation may be associated with altered network connectivity, surprisingly little is known about potential alterations in connectivity between these regions in the context of reward processing, although altered connectivity in OCD has been reported in association with other processes<sup>14,15</sup> or during the resting state.<sup>16</sup> To our knowledge, only 2 studies have investigated connectivity in association with the processing of reward in OCD.<sup>17,18</sup> In the first study, patients with OCD showed decreased functional connectivity between the ventral striatum (i.e., nucleus accumbens) and limbic areas, such as the amygdala, and increased functional connectivity between the ventral striatum (i.e., nucleus accumbens) and posterior insula, cerebellum, calcarine and temporal pole during reward anticipation, apart from mainly decreased connectivity during loss anticipation. The second study, a recent one by our group investigating functional connectivity during reward processing in an OCD sample partly overlapping with the current one, showed stronger functional connectivity between the posterior cingulate and the ventromedial prefrontal cortex (vmPFC) in patients compared with controls. These findings provide first evidence that abnormal connectivity between core regions involved in the processing of reinforcement and reward may constitute a central mechanism of OCD psychopathology.

Against this background, the present study used a reward-based learning task to explore potential alterations in connectivity during reward processing in a relatively large sample of patients with OCD and healthy controls. To obtain more specific information on the connectivity within relevant networks, in the present study we investigated effective connec-

tivity that, as opposed to the method of functional connectivity, provides additional information on direct influences between neuronal populations within the modelled network. Based on the current literature we expected connectivity alterations between regions previously reported to show alterations in activation in patients with OCD in the context of reward processing (i.e., mainly frontostriatal regions and the OFC), though not exclusively.

## Methods

### *Participants*

We recruited patients with OCD and healthy controls matched for age and sex to participate in this study. Patients were recruited from the inpatient hospital ward specialized in OCD of the Windach Institute and Hospital of Neurobehavioural Research and Therapy, Germany. Healthy volunteers were recruited from the community of the Klinikum rechts der Isar, Technical University of Munich, and through local advertisements. Exclusion criteria for both groups were a history of clinically important head injuries, seizures or neurologic diseases. Healthy controls with a history of psychiatric illness were excluded.

Handedness was assessed using Annett's questionnaire.<sup>19</sup> The diagnosis of OCD was established by an experienced psychiatrist based on DSM-IV criteria. We assessed OCD symptom severity using the Yale–Brown Obsessive Compulsive Scale (Y-BOCS;<sup>20</sup>). The Beck Depression Inventory (BDI) was used for determining potential presence of depressive symptoms.<sup>21</sup> Patients taking medication and with comorbidities were included, provided that OCD was the primary diagnosis.

All participants gave written informed consent to the study protocol. The protocol was developed in accordance with the Declaration of Helsinki and was approved by the ethics committee of the School of Medicine, Technical University of Munich.

### *Experimental design*

We used the Presentation software package (Neurobehavioural Systems Inc.) to project the stimuli on a screen inside the MRI scanner that could be viewed by participants through a mirror system. The task was similar to that described by Koch and colleagues.<sup>22</sup> Stimuli consisted of a card containing a geometrical figure: a cross, a half-moon, a triangle or a pentagon. Each figure predicted a number higher or lower than 5, with a probability of either 50% or 100%. Participants were asked to guess whether the figure on the card predicted a value higher or lower than 5. Though participants were informed about the different probabilities, they were unaware of the exact probability of each contingency. Each correct/incorrect response was rewarded/charged with €0.5, respectively. Thus, the task had a probabilistic character in order to investigate the extent to which reward processing was affected by reward probability.

An experimental run was completed after 64 trials, with 32 trials for each probability condition. As shown in Figure 1, each trial started with the presentation of the stimulus for 1.5 s, followed by the presentation of a question mark for 2.5 s during which participants indicated their response by button press. Feedback was provided in the following 2.5 s, and finally an interstimulus interval of 3.5 s was introduced before the following trial was presented. Participants were paid according to their performance, but a minimum of €20 was guaranteed for participation. Overall scanning time was 10 min.

### Functional MRI data acquisition and processing

Functional MRIs were acquired in a 3 T whole-body scanner (Achieva, Philips) using an 8-channel phased-array head coil. The data consisted of 644 scans, which were collected using a gradient echo echo-planar imaging sequence with the following parameters: echo time (TE) 30 ms, repetition time (TR) 2000 ms, flip angle 90°, field of view 192 × 192 × 122 mm, matrix 64 × 64, 37 slices, slice thickness 3 mm, and interslice gap 0 mm.

High-resolution, anatomical  $T_1$ -weighted scans were obtained using a magnetization-prepared rapid acquisition gradient echo (MPRAGE) sequence with the following scanning parameters: TR 9 ms, TE 4 ms, inversion time 1000 ms, flip angle 8°, matrix size 240 × 240 mm<sup>2</sup>, 170 slices, acceleration factor (SENSE) 2 with an isotropic resolution of 1 × 1 × 1 mm<sup>3</sup>.

Images were processed and statistical analysis was performed with SPM 12 ([www.fil.ion.ucl.ac.uk/spm](http://www.fil.ion.ucl.ac.uk/spm); Wellcome Trust Centre for Neuroimaging, University College London) in MATLAB 8.2.0 (R2015a, Mathworks). Preprocessing started with scan realignment to the mean image of every session, unwarping and linear and nonlinear normalization to the Montreal Neurological Institute (MNI) reference brain (MNI 152). The 6 head movement parameters were computed using the realignment algorithm and examined on a participant-by-participant basis. Participants with motion artifacts larger than 3 mm were excluded from further analyses. Data were then spatially smoothed using an isotropic Gaussian kernel (8 mm, full-width at half-maximum) and high-pass filtered with a 128 s cut-off.

### General linear model analysis

We used the general linear model (GLM) at first level to calculate statistical parametric maps of  $t$  statistics at the voxel

level. The onsets of each event, each with a variable duration of 1.5 s for stimulus presentation and 2.5 s for feedback and reward presentation, were convolved with a canonical hemodynamic response function (HRF). These modelled HRFs were then used as regressors within the GLM. Regressors of interest included the stimulus encoding (cross, half-moon, triangle or pentagon), the stimuli probabilities (50% and 100%) and the feedback (positive or negative). Individual movement parameters were also included as regressors of no interest.

A full factorial model was then generated at the group level to identify regions of interest to be included in dynamic causal modelling (DCM). These were regions activated for both positive and negative feedback ( $f$ -contrast,  $p < 0.05$  family-wise error [FWE]-corrected), since statistical maps obtained from positive feedback overlapped with those obtained from the negative feedback condition (i.e., no activated regions after the  $t$  contrasts positive > negative and negative > positive,  $p < 0.05$  FWE-corrected for control group and for patient group separately). The same procedure was performed for the patient and control groups. Regions were identified using the Anatomy toolbox for SPM.<sup>23–25</sup>

### Dynamic causal modelling

Hypothetical differences in the neuronal processing of positive/negative feedback between patients and controls were investigated by analyzing and comparing effective connectivity, indicating causal interactions in a proposed neuronal network involving regions known to be involved in feedback or reward processing. Effective connectivity was inferred using deterministic bilinear DCM.<sup>26,27</sup> This method simulates neuronal dynamics in a predefined neuronal network and how the dynamics change in response to experimental manipulations. Neuronal dynamics is inferred for a limited range of network models defined according to prior knowledge about the system being studied, and is characterized by distinct groups of parameters, described in 3 matrices: A, B and C. Matrix A contains the parameters describing endogenous connections between the volumes of interest; that is, describing the effects between the regions of interest in the absence of experimental perturbations.<sup>26</sup> Parameters describing modulatory effects of external manipulations on the connections are described in matrix B and parameters characterizing the driving inputs into the network in matrix C.

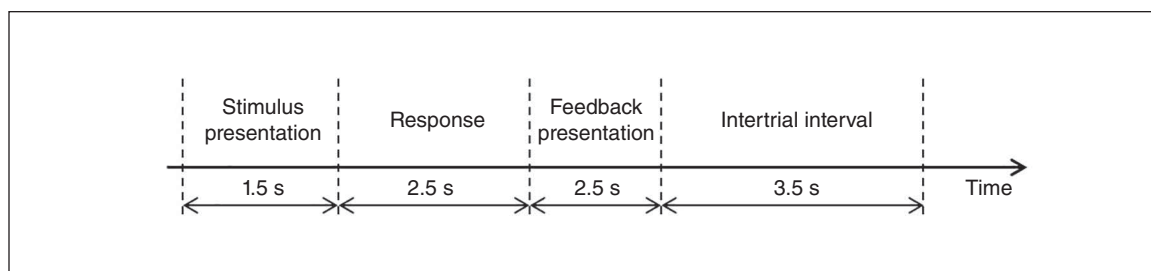


**Fig. 1:** Experimental design.

### Regions of interest for the DCM analysis

Volumes of interest (VOI) were selected based on 1) the statistical parametric maps generated after full factorial second-level analysis for both positive and negative feedback (*f*-contrast,  $p < 0.05$  FWE-corrected) both for the control and patient group, and 2) on networks assumed to be relevant for the pathophysiology of OCD and/or the processing of reward that have been frequently reported in OCD studies.<sup>1,10,28</sup> These regions are the right and left OFC; the right and left insula; the right and left dorsal striatum/putamen; the right and left visual cortex, considered here to be the region of input to the network as feedback was provided visually; and the vmPFC, connecting the subnetworks from the left and right hemispheres (Fig. 2). Connections with other VOIs were considered according to the available literature on reward processing.<sup>29</sup> Average MNI coordinates of the VOIs are shown in Table 1 and the localization of the average VOIs for the control group are illustrated in Figure 2.

For each participant, regional time series for each of the above-mentioned VOIs were extracted from 4 mm spheres centred on the activation maxima for the *f*-contrast “positive/negative feedback” ( $p < 0.001$ , uncorrected; when no time series could be defined, then the criterion  $p < 0.01$  or  $p < 0.05$  uncorrected was used) and that were located in the same anatomical region as indicated by the Anatomy toolbox for SPM.<sup>23–25</sup> Time series were adjusted for the effects of interest. Not all participants showed activation within the selected areas. Only those who showed activation maxima in all areas and for whom the network could be set up were included in DCM analysis: 30 patients with OCD and 37 control participants. All but 1 of these 30 patients and all healthy controls were part of a larger (44 patients, 37 controls), recently published study investigating seed-based functional connectivity.<sup>18</sup>

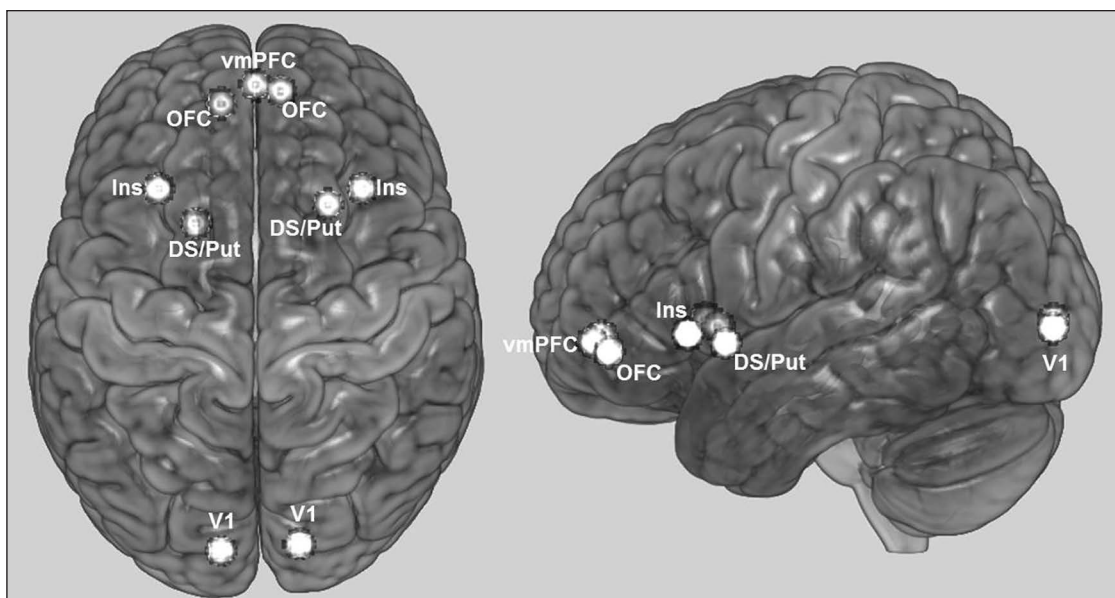
### Defining the model space

Figure 3 illustrates the base model from which the range of possible models evaluated in DCM was defined.<sup>29–35</sup> Intrinsic and modulatory connections are identified by dotted black and continuous black arrows, respectively. In the model shown here, external manipulations specifically affect the connection between the visual cortex and the OFC bilaterally. In this study, external manipulations correspond to the type of feedback received by participants (positive or negative). The model presented differs from the other models in the location of the modulatory effect. Assuming that the external manipulations can affect any of the 9 connections in the network (no distinction between left and right hemisphere), this makes 9 different possible models. Furthermore, assuming that modulation can affect differentially the forward or backward connection or both directions simultaneously, then the model space is composed by a total of 27 (i.e.,  $9 \times 3$ ) possible models. This number of possible models was finally reduced to 21 after removing the models that considered modulatory effects to occur on the forward and backward connections between the left and right OFC and insula (i.e., only bidirectional connectivity was assumed between the right and left OFC and between the right and left insula).

Each of the 21 models was computed on an individual level using the DCM12 analysis tool as implemented in SPM12.<sup>26,27</sup>

### Bayesian model selection

Models estimated on an individual level were then subjected to Bayesian model selection (BMS), a statistical tool that computes the probability of obtaining the measured data,  $y$ , given the model,  $m$ ; i.e., the model evidence,  $p(y|m)$ . The model chosen is that with highest log-evidence from the set of



**Fig. 2:** Localization of volumes of interest (VOIs) used in the dynamic causal modelling analysis. The regions illustrated correspond to 4 mm spheres at average Montreal Neurological Institute coordinates of the group of control participants. DS/Put = dorsal striatum/putamen; Ins = insula; OFC = orbitofrontal cortex; V1 = visual cortex; vmPFC = ventromedial prefrontal cortex.

21 possible models available.<sup>36,37</sup> In the present study, it is assumed that different neuronal dynamics underlie the different behavioural outcomes across participants and between groups, and therefore we used random-effects BMS.<sup>36</sup> The analysis was performed for the control and patient groups separately, and model selection was described in terms of exceedance probability for each model.

*Statistical analysis*

Since random-effects BMS yielded different optimal models for the 2 groups, comparison of connectivity parameters between patients and controls was performed on weighted parameters, derived after Bayesian model averaging (BMA).<sup>36,37</sup> Each connectivity parameter in BMA corresponds to a weighted average of that parameter across all models in the model space, with weights determined by the posterior probability of each model.

Reported below are the mean values for each endogenous (matrix A), modulatory (matrix B) and driving input (matrix C) connections for both control and test groups obtained after BMA. The latter retrieves the posterior mean and standard deviation for each parameter, and these were used to derive, for each parameter, the probability of the difference between the test and for the control groups. Correction for multiple comparisons — 41 for comparison of endogenous connections, 32 for modulatory and 2 for input — was performed by adapting the  $\alpha$  value according to the Holm–Bonferroni method.

Linear correlations between altered connectivity parameters and symptom severity, as measured by the YBOCS (total, obsessions, compulsions) and Obsessive–Compulsive Inventory (OCI), was explored using Pearson correlation and correcting for multiple comparisons with the Bonferroni method. Correlations were computed both taking into account values from all patients (medicated and unmedicated) as well as taking into account values from only medicated patients. The latter was done to assess potential effects of medication on neuronal dynamics. Owing to the small

**Table 1: Average MNI coordinates of the volumes of interest composing the analyzed network\***

VOI	Control			OCD		
	x	y	z	x	y	z
vmPFC	-0.32	54.65	-6.49	0.83	53.93	-6.07
IV1	-10.92	-92.76	1.08	-11.03	-94.41	-0.69
IOFC	-11.35	48.58	-8.19	-15.13	49.87	-9.27
IDS/Put	-19.11	11.5	-3.5	-18	13.85	0.59
lIns	-31.03	22.05	0.05	-31	22.93	-2.67
rV1	14.05	-90.59	1.20	13.17	-93.10	3.59
rOFC	8.4	52.8	-5.2	15.07	46.07	-7.93
rDS/Put	23.03	16.54	-2.76	22.69	17.10	-5.03
rIns	34.10	22.49	-2.27	36.2	22.53	-1.8

DS/Put = dorsal striatum/putamen; Ins = insula; l = left; MNI = Montreal Neurological Institute; OCD = obsessive–compulsive disorder; OFC = orbitofrontal cortex; r = right; V1 = visual cortex; vmPFC = ventromedial prefrontal cortex; VOI = volume of interest. \*Average was computed over all participants in each group.

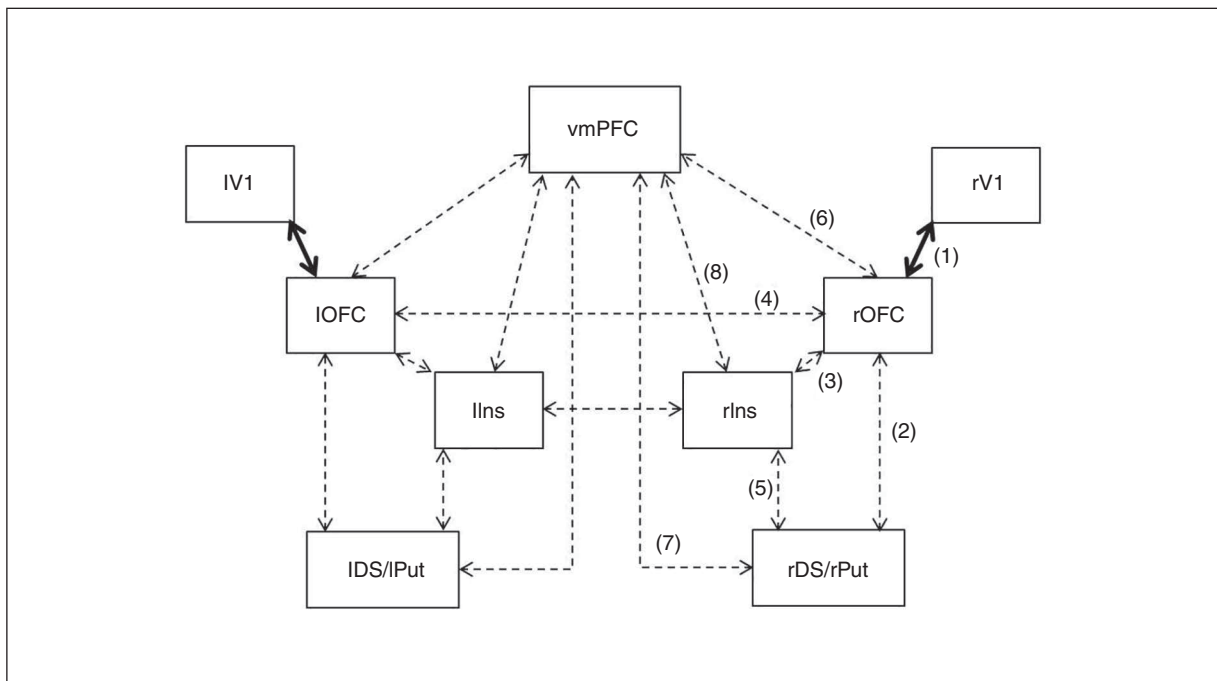


**Fig. 3:** One of the 21 models constituting the model space, in this case with the modulatory effect between visual cortex and OFC for both forward and backward direction. The connections considered are backed up by previous anatomic studies, as indicated by the numbers 1,<sup>30,31</sup> 2–4,<sup>32</sup> 5,<sup>33</sup> 6,<sup>34</sup> 7<sup>29</sup> and 8.<sup>29,35</sup> DS/Put = dorsal striatum/putamen; Ins = insula; l = left; OFC = orbitofrontal cortex; r = right; V1 = visual cortex; vmPFC = ventromedial prefrontal cortex.

number of unmedicated patients, no correlations could be computed separately for this subgroup. All statistical tests were performed with the statistics toolbox of MATLAB R2015b.

## Results

### Participants

Our sample included 37 patients with OCD and 39 healthy controls. All participants were right-handed. Participant characteristics are described in Table 2.

### Dynamic causal modelling

#### Model selection

The model with highest exceedance probability for the control group was model 1 (exceedance probability 55%), describing an effect of modulation at the forward connection between the visual cortex and the OFC. For the OCD group, the winning model was model 3 (exceedance probability 89%), for which the modulatory effect influenced both the forward and backward connections between the visual cortex and OFC (Fig. 4). Given that the winning model was different for both groups, statistical comparison of effective connectivity between the 2 groups was based on average parameters estimates derived after BMA.<sup>37</sup>

#### Differences in effective connectivity

Table 3 contains group average estimates of endogenous connectivity parameters (matrix A in DCM) inferred after BMA. Statistically significant differences were found after correcting for multiple comparisons for parameters describing influences between the following VOIs: between the vmPFC and the left and right OFC in both forward ( $\text{diff}_{\text{PFC} > \text{OFC}} = -0.095, p < 0.001$ ;  $\text{diff}_{\text{PFC} > \text{rOFC}} = -0.0714, p < 0.003$ ) and backward directions ( $\text{diff}_{\text{OFC} > \text{PFC}} = 0.1053, p < 0.001$ ;  $\text{diff}_{\text{OFC} > \text{rPFC}} = -0.0653, p < 0.005$ ), between the left visual cortex and left OFC for both forward ( $\text{diff}_{\text{IVI} > \text{OFC}} = -0.0318, p < 0.002$ ) and backward directions ( $\text{diff}_{\text{OFC} > \text{IVI}} = 0.0734, p < 0.002$ ), from the right OFC to the right visual cortex ( $\text{diff}_{\text{OFC} > \text{rVI}} = 0.171, p < 0.0001$ ), from the right OFC to the left OFC ( $\text{diff}_{\text{OFC} > \text{lOFC}} = 0.099, p < 0.0001$ ), from the right insula to the left insula ( $\text{diff}_{\text{Ins} > \text{lIns}} = 0.0726, p < 0.002$ ) and within the left visual cortex ( $\text{diff}_{\text{IVI} > \text{IVI}} = -0.1318, p < 0.0001$ ).

Statistically significant differences between patients and controls were obtained for the following positive feedback-related connectivity parameters (matrix B, Table 4): from the vmPFC to the left OFC (mean difference =  $-0.1325, p < 0.006$ ) and to the right OFC (mean difference =  $-0.1395, p < 0.008$ ). Significant differences were also found, independent of type of feedback, from the left visual cortex to the left OFC (positive: mean difference =  $0.1631, p < 0.001$ ; negative: mean difference =  $-0.2412, p < 0.001$ ), from the left to the right insula (positive: mean difference =  $-0.1084, p < 0.001$ ; negative: mean difference =  $-0.0938, p < 0.007$ ), from the right to the left OFC (positive: mean difference =  $0.0843, p < 0.002$ ; negative: mean difference =  $-0.0811, p < 0.002$ ). In addition to these, a significant difference was found for negative feedback-related

connectivity from the left to the right OFC (mean difference =  $-0.0656, p < 0.008$ ).

Finally, significant differences between the groups were observed in terms of input parameters (matrix C in DCM; Table 5) for the left visual cortex for negative feedback only (mean difference =  $0.2304, p < 0.001$ ) and for the right visual cortex for both positive and negative feedback (positive: mean difference =  $0.165, p < 0.001$ ; negative: mean difference =  $0.2989, p < 0.001$ ).

#### Correlation between effective connectivity parameters and clinical scores

Significant correlations (after Bonferroni correction) were found between the parameter describing the effect of the input in the left visual cortex and the severity of compulsions, when all patients, medicated and unmedicated, were considered ( $r = 0.44, p < 0.0141$ ; Fig. 5A); the severity of compulsions when only the 19 medicated patients were considered ( $r = 0.66, p < 0.0023$ ; Fig. 5B); and the OCI level obtained for the 19 medicated patients only ( $r = 0.54, p < 0.0178$ ; Fig. 5C). No correlations between the effect of the input on the left visual cortex (C-parameter) with age of onset or with the time since onset were found.

**Table 2: Demographic and clinical characteristics of study participants**

Characteristic	Group; mean $\pm$ SD*	
	OCD <i>n</i> = 37	Control <i>n</i> = 39
Sex, male:female	14:23	16:23
Age, yr	33.7 $\pm$ 10.1	32.2 $\pm$ 8.3
Medication, yes:no	24:13	—
Medication type, no. of patients†		
SSRI	16	—
SNRI	2	—
Tricyclic antidepressant	3	—
Benzodiazepine	1	—
NDRI	1	—
Atypical antipsychotic	1	—
Comorbidities, present:not present	22:15	—
Comorbidity, no. of patients‡		
Depression	18	—
Anxiety disorder	6	—
Personality disorder	2	—
Y-BOCS		
Total score	19.5 $\pm$ 6.4	—
Obsessions	10.1 $\pm$ 3.7	—
Compulsions	9.4 $\pm$ 3.8	—
BDI	16.6 $\pm$ 11.1	—
Age of onset, yr	15.9 $\pm$ 6.4	—
Time since onset, yr	17.7 $\pm$ 10.4	—

BDI = Beck Depression Inventory; NA = not applicable; NDRI = norepinephrine-dopamine reuptake inhibitor; SD = standard deviation; SNRI = serotonin-norepinephrine reuptake inhibitor; SSRI = selective serotonin reuptake inhibitor; Y-BOCS = Yale-Brown Obsessive Compulsive Scale.

\*Unless indicated otherwise.

†Two patients were taking more than 1 medication.

‡Three patients had more than 1 comorbidity.

**Discussion**

Dynamic causal modelling is a generic method to infer effective connectivity in a dynamic system, such as a neuronal circuit, from experimental measures of brain activity, in this case fMRI as an indirect measure of brain activity. Effective connectivity between 2 neuronal populations reflects how the activity of one population affects the activity of the other, expressed in units of rate (Hz), and how this interaction is affected by external stimulation.<sup>26,37</sup>

In the present study, DCM of neuronal activity associated with a reward learning task showed altered neuronal dynamics in parts of the frontostriatal system; i.e., mainly the vmPFC and the OFC, in patients with OCD compared with healthy controls. In particular, alterations in the influence of the vmPFC on both the left and right OFC were found for

endogenous connectivity and also for task-related connectivity. Average endogenous parameters were positive in both groups but larger in the patient group, which suggests a stronger effective connectivity between these areas in the OCD group. Similar to the present findings, we also detected an increased reward-related connectivity of the vmPFC in a recent study in patients with OCD compared with controls.<sup>18</sup> It should be noted that here, in an analysis performed independently from the previous one and by a different researcher, we analyzed effective connectivity, which investigates the directional influence different regions exert on each other under external stimulation. Therefore, the analysis performed in the present work provides supplementary information to that obtained with functional connectivity analysis. Although the results presented here are more complex, they are partly consistent with the increased connectivity between

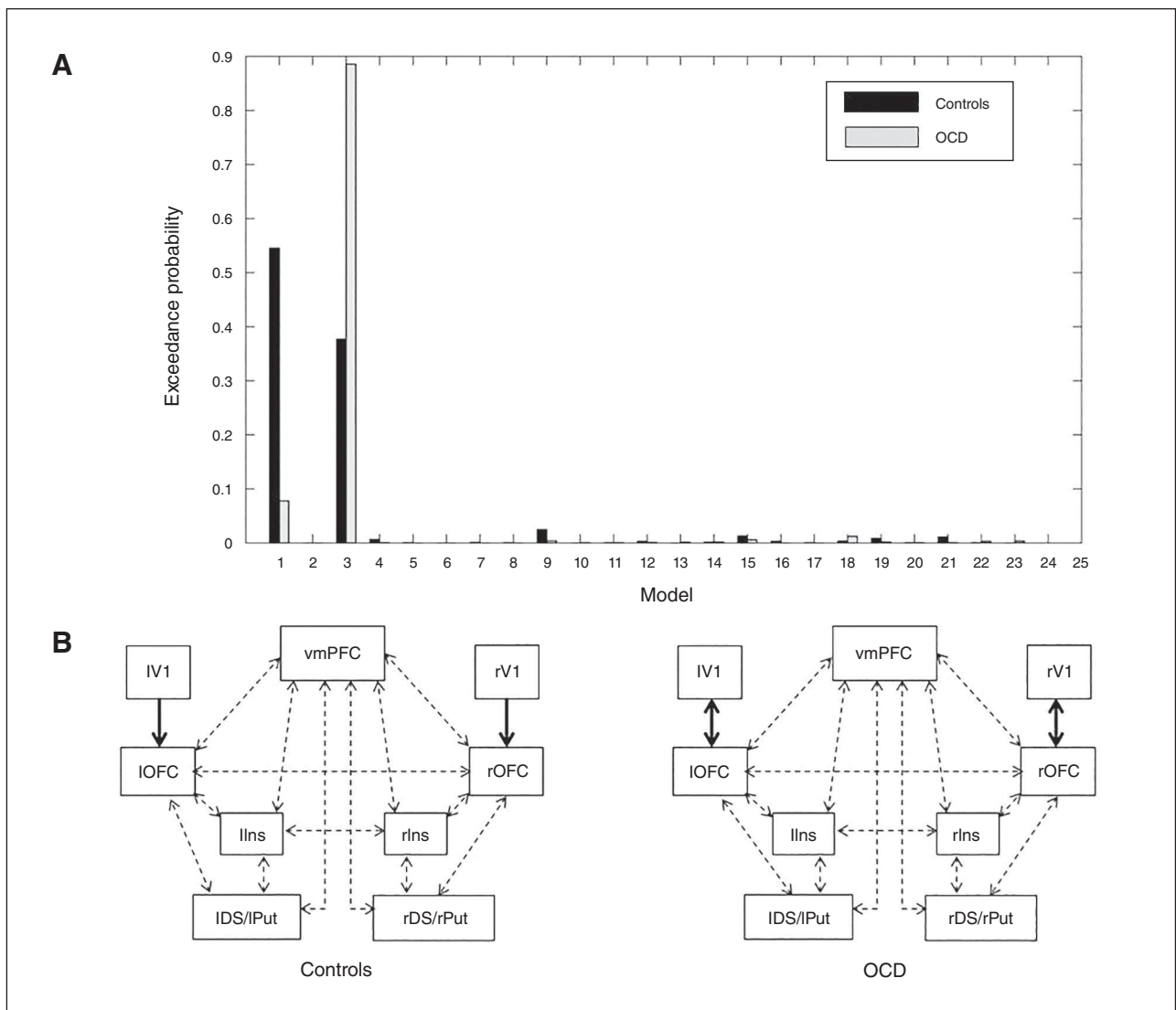


**Fig. 4:** (A) Model exceedance probabilities. (B) Winning model (highest exceedance probability) for patients with OCD (model 3) and control (model 1) groups. DS/Put = dorsal striatum/putamen; Ins = insula; l = left; OCD = obsessive-compulsive disorder; OFC = orbito-frontal cortex; r = right; V1 = visual cortex; vmPFC = ventromedial prefrontal cortex.

the vmPFC and the posterior cingulate cortex (PCC)<sup>18</sup> found with functional connectivity analysis, also for the positive feedback condition. The vmPFC constitutes a central component of the default mode network, an intrinsic brain network that is assumed to be active when a person is thinking about himself instead of the outside world.<sup>38</sup> A recent comprehensive meta-analysis of resting state functional connec-

tivity in OCD illustrated the central role that the vmPFC plays in the context of the disorder. It showed a dysconnectivity within the default mode network peaking in the anterior cingulate cortex (ACC) and the vmPFC in adult patients with OCD.<sup>39</sup> Considering that the vmPFC is assumed to be predominantly responsible for the processing of internal mental states and events, its increased effective connectivity

**Table 3: Group average endogenous parameters (matrix A) in Hz**

Connection	Control	OCD	Controls – OCD		
			Difference mean	Difference SD	1 – $p^*$
vmPFC to vmPFC	-0.1164	-0.1387	0.0224	0.0294	0.7767
vmPFC to IOFC	<b>0.0095</b>	<b>0.1045</b>	<b>-0.095</b>	<b>0.0249</b>	<b>0.9999</b>
vmPFC to IDS/Put	0.0242	0.0218	0.0024	0.0223	0.543
vmPFC to lIns	-0.0325	-0.0576	0.0251	0.0235	0.8578
vmPFC to rOFC	<b>0.0041</b>	<b>0.0756</b>	<b>-0.0714</b>	<b>0.0255</b>	<b>0.9974</b>
vmPFC to rDS/Put	0.0457	0.021	0.0247	0.0217	0.8734
vmPFC rIns	0.0199	0.0084	0.0115	0.024	0.6839
IV1 to IV1	<b>-0.3203</b>	<b>-0.1885</b>	<b>-0.1318</b>	<b>0.0227</b>	<b>1</b>
IV1 to IOFC	<b>0.0075</b>	<b>0.0393</b>	<b>-0.0318</b>	<b>0.011</b>	<b>0.9982</b>
IOFC to vmPFC	<b>0.1525</b>	<b>0.0472</b>	<b>0.1053</b>	<b>0.0246</b>	<b>1</b>
IOFC to IV1	<b>0.1426</b>	<b>0.0692</b>	<b>0.0734</b>	<b>0.0252</b>	<b>0.9982</b>
IOFC to IOFC	-0.0795	-0.0627	-0.0167	0.0291	0.7175
IOFC to IDS/Put	0.1003	0.0618	0.0385	0.022	0.9603
IOFC lIns	0.0399	0.031	0.0089	0.0237	0.6464
IOFC rOFC	0.0566	0.0032	0.0534	0.0253	0.9826
IDS/Put to vmPFC	0.0463	0.0149	0.0314	0.0286	0.8643
IDS/Put to IOFC	0.0154	0.0445	-0.0291	0.0289	0.8427
IDS/Put to IDS/Put	-0.0479	-0.0626	0.0147	0.0295	0.6906
IDS/Put to lIns	0.0449	0.0275	0.0175	0.0275	0.7377
lIns to vmPFC	0.0377	-0.0035	0.0412	0.028	0.929
lIns to IOFC	0.0624	0.0351	0.0273	0.0273	0.8414
lIns to IDS/Put	0.0927	0.0902	0.0025	0.0259	0.539
lIns to lIns	-0.0748	-0.0683	-0.0065	0.0299	0.5865
lIns to rIns	0.1088	0.0814	0.0274	0.0273	0.842
rV1 to rV1	-0.2492	-0.2393	-0.0098	0.023	0.6656
rV1 to rOFC	0.0287	0.0271	0.0016	0.0116	0.5558
rOFC to vmPFC	<b>0.1187</b>	<b>0.1841</b>	<b>-0.0653</b>	<b>0.025</b>	<b>0.9955</b>
rOFC to IOFC	<b>0.0954</b>	<b>-0.0036</b>	<b>0.099</b>	<b>0.0254</b>	<b>1</b>
rOFC to rV1	<b>0.1325</b>	<b>-0.0385</b>	<b>0.171</b>	<b>0.0251</b>	<b>1</b>
rOFC to rOFC	-0.0917	-0.0894	-0.0023	0.0297	0.531
rOFC to rDS/Put	0.0793	0.0459	0.0334	0.0227	0.9294
rOFC to rIns	0.0278	-0.0195	0.0473	0.0236	0.9777
rDS/Put to vmPFC	0.0434	0.0496	-0.0063	0.0288	0.5863
rDS/Put to rOFC	0.0439	0.0346	0.0093	0.0303	0.6205
rDS/Put to rDS/Put	-0.0537	-0.0493	-0.0044	0.0299	0.5588
rDS/Put to rIns	0.049	0.0696	-0.0205	0.0284	0.7655
rIns to vmPFC	0.0417	0.0983	-0.0566	0.027	0.982
rIns to lIns	<b>0.1281</b>	<b>0.0555</b>	<b>0.0726</b>	<b>0.0248</b>	<b>0.9983</b>
rIns to rOFC	0.0671	0.0822	-0.0151	0.0264	0.7158
rIns to rDS/Put	0.0819	0.0627	0.0192	0.0253	0.7763
rIns to rIns	0.0898	-0.0719	-0.0179	0.0298	0.726

DS/Put = dorsal striatum/putamen; Ins = insula; l = left; OCD = obsessive-compulsive disorder; OFC = orbitofrontal cortex; r = right; SD = standard deviation; V1 = visual cortex; vmPFC = ventromedial prefrontal cortex.

\*Posterior probabilities of the parameter difference. Text in bold indicates a significant difference from zero, after applying the Holm-Bonferroni correction for multiple comparisons.

to the OFC in the patient group in the present context might reflect excessive internal, self-related processing impairing normal responsiveness toward external rewards and incentives. This may explain the constant need for additional rewarding stimulation reflected in the incapacity to suppress

compulsive behaviours. Interestingly, increased connectivity of the vmPFC has also been observed in patients with psychosis both during rest<sup>40</sup> and during tasks (e.g., in association with a self-reflection task).<sup>41</sup> Hence, altered vmPFC connectivity might constitute a common neuropathological

**Table 4: Group average modulation parameters (matrix B), strength in HZ**

Connection	Control		OCD		Control – OCD					
					+Feedback			–Feedback		
	+Feedback	–Feedback	+Feedback	–Feedback	Mean	SD	1 – p*	Mean	SD	1 – p*
vmPFC to IOFC	–0.0451	0.0521	0.0874	0.0716	<b>–0.1325</b>	<b>0.0523</b>	<b>0.9944</b>	–0.0194	0.0577	0.6318
vmPFC to IDS/Put	–0.0211	0.0381	–0.0827	–0.0156	0.0616	0.0498	0.8921	0.0537	0.0486	0.8653
vmPFC to llns	0.0315	0.0706	–0.0177	–0.0198	0.0492	0.0432	0.8727	0.0904	0.0589	0.9377
vmPFC to rOFC	–0.0553	0.0720	0.0842	–0.0370	<b>–0.1395</b>	<b>0.0575</b>	<b>0.9924</b>	0.1089	0.0721	0.9345
vmPFC to rDS/Put	–0.0186	0.0218	0.0085	0.0492	–0.0272	0.0511	0.7024	–0.0274	0.0475	0.7180
vmPFC to rlns	–0.0795	–0.0108	–0.0146	0.0003	–0.0649	0.0554	0.8790	–0.0111	0.0580	0.5759
IV1 to IOFC	0.1267	–0.1774	–0.0364	0.0638	<b>0.1631</b>	<b>0.0365</b>	<b>1.0000</b>	<b>–0.2412</b>	<b>0.0609</b>	<b>1.0000</b>
IOFC to vmPFC	0.0229	0.0645	–0.0044	0.0168	0.0273	0.0751	0.6419	0.0477	0.0744	0.7393
IOFC to IV1	–0.0205	0.0129	0.1129	–0.1459	–0.1335	0.1299	0.8480	0.1588	0.1276	0.8934
IOFC to IDS/Put	–0.0502	–0.0392	–0.0051	–0.0011	–0.0451	0.0422	0.8576	–0.0381	0.0435	0.8095
IOFC to llns	–0.0858	–0.0779	–0.0580	0.0196	–0.0278	0.0524	0.7022	–0.0975	0.0471	0.9807
IOFC to rOFC	0.0001	0.0000	0.0046	0.0656	–0.0044	0.0245	0.5716	<b>–0.0656</b>	<b>0.0270</b>	<b>0.9924</b>
IDS/Put to vmPFC	0.0012	0.0155	0.0342	–0.0855	–0.0330	0.0547	0.7268	0.1010	0.0501	0.9782
IDS/Put to IOFC	0.0001	0.0001	0.0044	0.0033	–0.0043	0.0248	0.5690	–0.0032	0.0226	0.5559
IDS/Put to llns	–0.0414	–0.0100	0.0021	–0.0079	–0.0436	0.0531	0.7941	–0.0021	0.0413	0.5204
llns to vmPFC	–0.0529	0.1088	0.0015	0.0027	–0.0544	0.0454	0.8848	0.1062	0.0506	0.9820
llns to IOFC	–0.0284	0.0486	0.0780	–0.0415	–0.1064	0.0596	0.9628	0.0900	0.0545	0.9508
llns to IDS/Put	0.0623	0.0138	–0.0073	0.0038	0.0697	0.0537	0.9028	0.0100	0.0385	0.6028
llns to rlns	–0.0002	–0.0001	0.1082	0.0937	<b>–0.1084</b>	<b>0.0320</b>	<b>0.9996</b>	<b>–0.0938</b>	<b>0.0295</b>	<b>0.9993</b>
rV1 to rOFC	0.0788	–0.1125	0.0063	–0.2692	0.0724	0.0428	0.9547	0.1567	0.0707	0.9866
rOFC to vmPFC	–0.0138	0.0190	–0.0462	0.0566	0.0324	0.0720	0.6737	–0.0377	0.0894	0.6633
rOFC to IOFC	—	–0.0002	–0.0843	0.0809	<b>0.0843</b>	<b>0.0283</b>	<b>0.9986</b>	<b>–0.0811</b>	<b>0.0281</b>	<b>0.9980</b>
rOFC to rV1	0.0251	0.0203	–0.0068	–0.0524	0.0319	0.1280	0.5985	0.0726	0.1275	0.7156
rOFC to rDS/Put	0.0869	0.0691	–0.0028	0.0000	0.0897	0.0617	0.9272	0.0691	0.0474	0.9277
rOFC to rlns	0.0224	–0.0962	0.0697	–0.0184	–0.0473	0.0693	0.7523	–0.0779	0.0488	0.9446
rDS/Put to vmPFC	0.023	0.0190	–0.0281	0.0926	0.0510	0.0528	0.8332	–0.0736	0.0483	0.9360
rDS/Put to rOFC	0	0	0.0079	0.0030	–0.0079	0.0293	0.6063	–0.0030	0.0240	0.5489
rDS/Put to rlns	–0.0155	0.0047	–0.0119	–0.0094	–0.0036	0.0569	0.5252	0.0140	0.0469	0.6178
rlns to vmPFC	–0.0259	0.0364	0.0051	0.0043	–0.0311	0.0427	0.7666	0.0320	0.0459	0.7576
rlns to llns	–0.0001	0.0000	0.0265	0.0690	–0.0266	0.0336	0.7858	–0.0690	0.0420	0.9499
rlns to rOFC	–0.0892	–0.0493	–0.0516	–0.0318	–0.0375	0.0617	0.7284	–0.0175	0.0450	0.6514
rlns to rDS/Put	–0.0003	0.0427	0.0041	0.0066	–0.0044	0.0404	0.5434	0.0361	0.0437	0.7959

DS/Put = dorsal striatum/putamen; lns = insula; l = left; OCD = obsessive-compulsive disorder; OFC = orbitofrontal cortex; r = right; SD = standard deviation; V1 = visual cortex; vmPFC = ventromedial prefrontal cortex.

\*Posterior probabilities of differences were corrected (Holm-Bonferroni) for multiple comparisons. Text in bold indicates a parameter difference significantly different from zero.

**Table 5: Group average input parameters (matrix C), strength in Hz\***

Input	Controls		OCD		Controls – OCD					
					Positive feedback			Negative feedback		
	Positive	Negative	Positive	Negative	Difference mean	Difference SD	1 – p	Difference mean	Difference SD	1 – p
IV1	1.4195	1.3098	1.3489	1.0795	0.0706	0.0366	9.73E <sup>-01</sup>	<b>0.2304</b>	<b>0.0449</b>	<b>1</b>
rV1	1.5021	1.3457	1.3369	1.0468	<b>0.165</b>	<b>0.0417</b>	<b>1.00E<sup>+00</sup></b>	<b>0.2989</b>	<b>0.0434</b>	<b>1</b>

l = left; OCD = obsessive-compulsive disorder; SD = standard deviation; V1 = visual cortex.

\*Text in bold indicates a parameter difference significantly different from zero.

mechanism that might not only account for the frequent occurrence of OCD symptoms in psychosis, but also might also explain why both patient groups suffer from an exces-

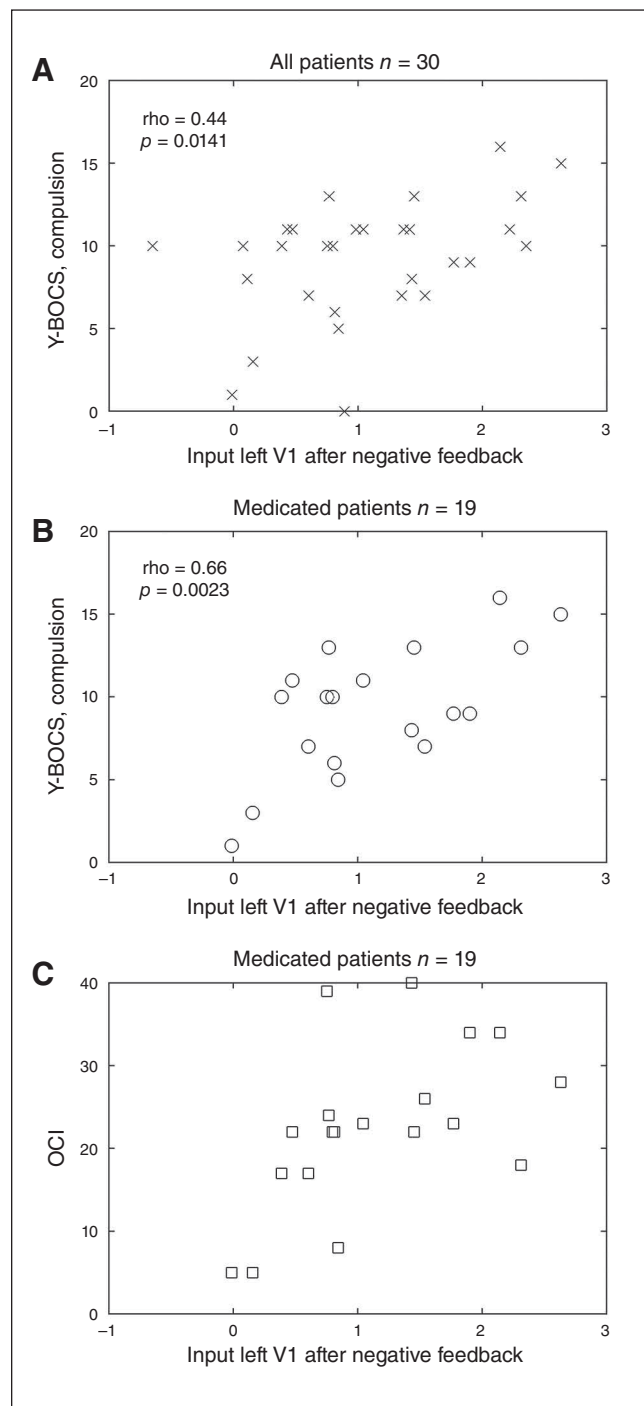


**Fig. 5:** (A) Compulsion measure of Y-BOCS as a function of input effect on the left visual cortex for negative feedback in all patients, and (B) in medicated patients only. (C) OCI as a function of input effect on the left visual cortex for negative feedback and for medicated patients only. OCI = Obsessive–Compulsive Inventory; V1 = visual cortex; Y-BOCS = Yale–Brown Obsessive–Compulsive Scale.

sive internal self-related processing at the expense of recognizing and internalizing external facts and evidence.

When taking a closer look at the connectivity parameters, we notice that average parameters derived from positive feedback conditions were negative for the control group and positive for patients with OCD. Parameters derived for negative feedback conditions were not significantly different between the 2 groups. Negative parameters indicate that neuronal activity in the vmPFC induces a decrease in neuronal activity in the OFC and vice versa. Hence, these results point to a smaller inhibitory influence of the vmPFC, known to exert inhibitory effects on networks involved in mainly emotional processing,<sup>42,43</sup> on the OFC in patients relative to controls under positive feedback conditions. The OFC constitutes the final common pathway of the cortico–striato–thalamo–cortical (CSTC) system.<sup>7</sup> Within this system it is possible to distinguish 2 main pathways: the direct loop, constituting a positive feedback loop, and the indirect loop, representing a negative feedback loop.<sup>7</sup> According to the CSTC model of OCD, patients suffer from an imbalanced activation of the direct and the indirect loop<sup>7,44</sup> in terms of an excessive activation of the excitatory positive feedback loop (direct loop). Consequently, the indirect loop is no longer able to regulate the activity of the direct pathway, resulting in an increased cortical, or more specifically OFC, activation. The present findings extend this model by indicating that, under certain conditions, a decreased inhibitory influence of the vmPFC on the OFC might likewise underlie excessive OFC activation in patients with OCD. Whether this excessive OFC activation and altered connectivity to the vmPFC in patients with OCD plays a role in the context of compulsive behaviour and the affective processes going along with it as well as which of the 2 mechanisms is the predominant cause of the frequently reported excessive OFC activation in patients with OCD remain to be clarified.

Moreover, our results show different effects of input in sensory areas between patients and controls, a finding that might emphasize the assumption of a deficient processing of the valence of external stimuli and rewards, as discussed earlier. Alterations in effective connectivity between the visual cortex and OFC, namely the mutual endogenous influence between the left visual cortex and the left OFC and the task-related connectivity from the left visual cortex to the left OFC for both positive and negative feedback suggest that sensitivity of sensory areas to positive or negative feedback is also influenced by its valence. The opposite sign of average parameters (Table 4) indicates that the modulatory effect induced by positive and negative feedback is different for both groups.

The correlation between the effect of negative input in the left visual cortex and behavioural measures of compulsion and OCI in medicated patients (Fig. 5) with higher levels of compulsion associated with larger effects of negative input in the left visual cortex, indicates that the differential impact of negative feedback in patients with OCD with regard to sensory areas might be of clinical relevance.<sup>45</sup> From a clinical perspective, one could assume that

a disrupted connectivity between regions involved in the sensory processing of external events may affect the ability to update internal reference frames and consequently induce an enhanced response to negative stimulus valence going along with compulsive behaviour.

### Limitations

Some limiting factors need to be addressed. First, we need to take into account that effective connectivity depends on the architecture of the network considered — in this case, on how many neuronal regions/nodes are considered and how they are interconnected — as well as on the nature of external manipulations.<sup>26,37</sup> That is why the specificity of the changes in connectivity that we found will likely differ depending on the nature of the task investigated as well as on the individual specificities of the condition. Hence, the results do not disregard the clinical relevance of other areas for OCD.

The nature of the task, together with the analysis performed, highlighted one of the several neuronal substrates that likely determine the clinical features of OCD. Additionally, the multitude of contexts in which the symptoms of OCD can manifest, with a multitude of experimental manipulation likely to induce measurable changes in neuronal dynamics, makes this condition particularly suitable to be addressed with DCM.

### Conclusion

Alterations in effective connectivity in parts of the default mode and frontostriatal networks in patients with OCD relative to healthy controls during a reward-learning task suggest a disruption in responses to external rewards in patients. This may underlie the urge for reinforcement and accompanying compulsive behaviour in OCD.

**Acknowledgement:** This work was supported by the German Research Foundation (DFG) and the Technical University of Munich within the funding programme Open Access Publishing.

**Affiliations:** From the Department of Neuroradiology, School of Medicine, Klinikum Rechts der Isar, Technical University of Munich, Munich, Germany (Rus, Reess, Wohlschläger, Koch); the TUM-Neuroimaging Center (TUM-NIC) School of Medicine of Klinikum rechts der Isar, Technische Universität München TUM, Ismaninger Strasse 22, 81675 Munich, Germany (Rus, Reess, Wohlschläger, Koch); the Research Unit of the Buhl-Strohmaier Foundation for Pediatric Neuroorthopaedics and Cerebral Palsy, Department of Orthopedics and Sports Orthopedics, School of Medicine, Klinikum Rechts der Isar, Technical University of Munich, Munich, Germany (Alves-Pinto); the Graduate School of Systemic Neurosciences GSN, Ludwig-Maximilians-Universität, Biocenter, Munich, Germany (Rus, Reess, Koch); the Department of Psychiatry and Psychotherapy, Jena University Hospital, Jena, Germany (Wagner); the Windach Institute and Hospital of Neurobehavioural Research and Therapy (WINTR), Windach, Germany (Berberich); and the Department of Neuroradiology, University of Zürich, Zürich, Switzerland (Rus).

**Funding:** This study was supported by a Deutsche Forschungsgemeinschaft grant to K. Koch (KO 3744/2-1) and G. Wagner (WA 3001/3-1).

**Competing interests:** None declared.

**Contributors:** O. Rus, G. Wagner, G. Berberich and K. Koch designed the study. O. Rus, T. Reess, G. Berberich and K. Koch acquired the data, which A. Alves-Pinto, A. Wohlschläger and K. Koch analyzed. A. Alves-Pinto and K. Koch wrote the article, which all authors reviewed. All authors approved the final version to be published and can certify that no other individuals not listed as authors have made substantial contributions to the paper.

### References

- Milad MR, Rauch SL. Obsessive-compulsive disorder: beyond segregated cortico-striatal pathways. *Trends Cogn Sci* 2012;16:43-51.
- Sescousse G, Caldú X, Segura B, et al. Processing of primary and secondary rewards: a quantitative meta-analysis and review of human functional neuroimaging studies. *Neurosci Biobehav Rev* 2013; 37:681-96.
- Berridge KC, Kringelbach ML. Pleasure systems in the brain. *Neuron* 2015;86:646-64.
- Denys D, Mantione M, Figee M, et al. Deep brain stimulation of the nucleus accumbens for treatment-refractory obsessive-compulsive disorder. *Arch Gen Psychiatry* 2010;67:1061-8.
- Huff W, Lenartz D, Schormann M, et al. Unilateral deep brain stimulation of the nucleus accumbens in patients with treatment-resistant obsessive-compulsive disorder: outcomes after one year. *Clin Neurol Neurosurg* 2010;112:137-43.
- Sturm V, Lenartz D, Koulousakis A, et al. The nucleus accumbens: a target for deep brain stimulation in obsessive-compulsive-and anxiety-disorders. *J Chem Neuroanat* 2003;26:293-9.
- Saxena S, Rauch SL. Functional neuroimaging and the neuroanatomy of obsessive-compulsive disorder. *Psychiatr Clin North Am* 2000;23:563-86.
- Jung W, Kang DH, Han J, et al. Aberrant ventral striatal responses during incentive processing in unmedicated patients with obsessive-compulsive disorder. *Acta Psychiatr Scand* 2011;123: 376-86.
- Figee M, Vink M, de Geus F, et al. Dysfunctional reward circuitry in obsessive-compulsive disorder. *Biol Psychiatry* 2011;69:867-74.
- Kaufmann C, Beucke J, Preuß F, et al. Medial prefrontal brain activation to anticipated reward and loss in obsessive-compulsive disorder. *Neuroimage Clin* 2013;2:212-20.
- Remijnse PL, Nielen MM, van Balkom AJ, et al. Reduced orbitofrontal-striatal activity on a reversal learning task in obsessive-compulsive disorder. *Arch Gen Psychiatry* 2006;63:1225-36.
- Marsh R, Tau GZ, Wang Z, et al. Reward-based spatial learning in unmedicated adults with obsessive-compulsive disorder. *Am J Psychiatry* 2015;172:383-92.
- Piras F, Piras F, Chiapponi C, et al. Widespread structural brain changes in OCD: a systematic review of voxel-based morphometry studies. *Cortex* 2015;62:89-108.
- Han H, Jung W, Yun J-Y, et al. Disruption of effective connectivity from the dorsolateral prefrontal cortex to the orbitofrontal cortex by negative emotional distraction in obsessive-compulsive disorder. *Psychol Med* 2016;46:921-32.
- Jhung K, Ku J, Kim SJ, et al. Distinct functional connectivity of limbic network in the washing type obsessive-compulsive disorder. *Prog Neuropsychopharmacol Biol Psychiatry* 2014;53:149-55.
- Peterson A, Thome J, Lanius RA. Resting-state neuroimaging studies: A new way of identifying differences and similarities among the anxiety disorders? *Can J Psychiatry* 2014;59:294.
- Jung WH, Kang D-H, Kim E, et al. Abnormal corticostriatal-limbic functional connectivity in obsessive-compulsive disorder during reward processing and resting-state. *Neuroimage Clin* 2013;3:27-38.
- Koch K, Reess TJ, Rus OG, et al. Increased default mode network connectivity in obsessive-compulsive disorder during reward processing. *Front Psychiatry* 2018;9:254.
- Annett M. A classification of hand preference by association analysis. *Br J Psychol* 1970;61:303-21.
- Goodman WK, Price LH, Rasmussen SA, et al. The Yale-Brown Obsessive Compulsive Scale: I. development, use, and reliability. *Arch Gen Psychiatry* 1989;46:1006-11.

21. Beck A, Ward C, Mendelson M, et al. An inventory for measuring depression. *Arch Gen Psychiatry* 1961;4:561-71.
22. Koch K, Wagner G, Schachtzabel C, et al. Association between white matter fiber structure and reward-related reactivity of the ventral striatum. *Hum Brain Mapp* 2014;35:1469-76.
23. Eickhoff SB, Paus T, Caspers S, et al. Assignment of functional activations to probabilistic cytoarchitectonic areas revisited. *Neuroimage* 2007;36:511-21.
24. Eickhoff SB, Stephan KE, Mohlberg H, et al. A new SPM toolbox for combining probabilistic cytoarchitectonic maps and functional imaging data. *Neuroimage* 2005;25:1325-35.
25. Eickhoff SB, Heim S, Zilles K, et al. Testing anatomically specified hypotheses in functional imaging using cytoarchitectonic maps. *Neuroimage* 2006;32:570-82.
26. Friston KJ, Harrison L, Penny WD. Dynamic causal modelling. *Neuroimage* 2003;19:1273-302.
27. Penny WD, Stephan KE, Mechelli A, et al. Modelling functional integration: a comparison of structural equation and dynamic causal models. *Neuroimage* 2004;23:264-74.
28. Becker MP, Nitsch AM, Schlösser R, et al. Altered emotional and BOLD responses to negative, positive and ambiguous performance feedback in OCD. *Soc Cogn Affect Neurosci* 2014;9:1127-33.
29. Gottfried JA. *Neurobiology of sensation and reward*. CRC Press; 2011.
30. Barbas H. Organization of cortical afferent input to orbitofrontal areas in the rhesus monkey. *Neuroscience* 1993;56:841-64.
31. Carmichael S, Price JL. Sensory and premotor connections of the orbital and medial prefrontal cortex of macaque monkeys. *J Comp Neurol* 1995;363:642-64.
32. Cavada C, Tejedor J, Cruz-Rizzolo RJ, et al. The anatomical connections of the macaque monkey orbitofrontal cortex. A review. *Cereb Cortex* 2000;10:220-42.
33. Chikama M, McFarland NR, Amaral DG, et al. Insular cortical projections to functional regions of the striatum correlate with cortical cytoarchitectonic organization in the primate. *J Neurosci* 1997;17:9686-705.
34. Calzavara R, Mailly P, Haber SN. Relationship between the corticostriatal terminals from areas 9 and 46, and those from area 8A, dorsal and rostral premotor cortex and area 24c: an anatomical substrate for cognition to action. *Eur J Neurosci* 2007;26:2005-24.
35. Carmichael S, Price J. Connectional networks within the orbital and medial prefrontal cortex of macaque monkeys. *J Comp Neurol* 1996;371:179-207.
36. Stephan KE, Penny WD, Daunizeau J, et al. Bayesian model selection for group studies. *Neuroimage* 2009;46:1004-17.
37. Stephan KE, Penny WD, Moran RJ, et al. Ten simple rules for dynamic causal modeling. *Neuroimage* 2010;49:3099-109.
38. Raichle ME. The brain's default mode network. *Annu Rev Neurosci* 2015;38:433-47.
39. Gürsel DA, Avram M, Sorg C, et al. Frontoparietal areas link impairments of large-scale intrinsic brain networks with aberrant fronto-striatal interactions in OCD: a meta-analysis of resting-state functional connectivity. *Neurosci Biobehav Rev* 2018;87:151-60.
40. Eryilmaz H, Tanner AS, Ho NF, et al. Disrupted working memory circuitry in schizophrenia: disentangling fMRI markers of core pathology vs other aspects of impaired performance. *Neuropsychopharmacology* 2016;41:2411.
41. Curcio-Blake B, van der Meer L, Pijnenborg GH, et al. Insight and psychosis: functional and anatomical brain connectivity and self-reflection in Schizophrenia. *Hum Brain Mapp* 2015;36:4859-68.
42. Quirk GJ, Beer JS. Prefrontal involvement in the regulation of emotion: convergence of rat and human studies. *Curr Opin Neurobiol* 2006;16:723-7.
43. Ochsner KN, Silvers JA, Buhle JT. Functional imaging studies of emotion regulation: a synthetic review and evolving model of the cognitive control of emotion. *Ann N Y Acad Sci* 2012;1251:E1-24.
44. Baxter LR Jr, Saxena S, Brody AL, et al., eds. Brain mediation of obsessive-compulsive disorder symptoms: evidence from functional brain imaging studies in the human and nonhuman primate. *Semin Clin Neuropsychiatry* 1996;1:32-47.
45. Stern ER, Welsh RC, Fitzgerald KD, et al. Hyperactive error responses and altered connectivity in ventromedial and fronto-insular cortices in obsessive-compulsive disorder. *Biol Psychiatry* 2011; 69:583-91.